Negative-Refractive Bicrystal with Broken Symmetry Produces Asymmetric Electromagnetic Fields in Guided-Wave Heterostructures

Clifford M. Krowne*

Microwave Technology Branch, Electronics Science & Technology Division, Naval Research Laboratory, Washington, D.C. 20375-5347, USA

(Received 16 December 2003; published 29 July 2004)

Heterostructure arrangements of uniaxial bicrystals have been discovered to produce electromagnetic fields with asymmetric distributions in guide wave structures. The property behind this remarkable phenomenon is the broken crystalline symmetry which allows the new physics to be seen in unsymmetric distributions. Here the theory behind this phenomenon is presented, numerical calculations are performed using an *ab initio* anisotropic Green's function approach, and the results provided at 10 GHz for a realistic crystal system with nominal permittivity of 5. Asymmetric distributions seen here are one facet of the broken symmetry property which generates negative refraction for impinging waves on a bicrystal.

DOI: 10.1103/PhysRevLett.93.053902 PACS numbers: 41.20.Jb, 84.40.–x

A recent finding [1] has shown that a uniaxial bicrystal (BC) shows negative refraction (which is also total); that is, exit rays present a bending opposite with respect to the normal compared to an ordinary right-handed medium (RHM) for certain incidence angles. A negative refractive (NR) property also occurs for a left-handed medium (LHM), and when its absolute values of constitutive constants are identical to those of the RHM, it also shows total refraction. In general, what is shared here between the bicrystal and the LHM is the negative refractive property. The NR property in the bicrystal arises from broken crystalline symmetry, and allows the interesting physics summarized above to be displayed. Rays being traced are power flow lines in the optics case, and have an analog, as pointed out in [1], of ballistic electron motion in a semiconductor heterostructure.

Very unusual field distributions have been discovered in guided wave LHM structures [2], with counterintuitive field line direction and circulation patterns. Broken crystal symmetry in a bicrystal not only produces NR, but also breaks field symmetry, allowing asymmetric distributions of electromagnetic fields in the cross section in which heterostructure layering occurs when guided-wave propagation is perpendicular to this cross section in a longitudinal direction. This latter physics property, asymmetry in the electromagnetic field distributions, hints at extremely important electronic properties in microwave and millimeter wave integrated circuits, already examined for isotropic LHM [3]. Individual heterostructure layers are not field symmetry breaking and do not lead to asymmetric field distributions. In fact, when a single crystal is inserted into a guiding structure, nothing special happens.

It is demonstrated in this Letter, for the first time, using a model stripline structure to guide the wave, that a bicrystal will indeed create asymmetric rf electric and magnetic field distributions. Calculations are done using an *ab initio* approach with an anisotropic Green's function which allows the physical properties of the uniaxial crystals to be treated through their tensors. The results have very important implications for microwave transmission devices which rely on asymmetric field distributions. In principal, there is no reason why this cannot be extended to optical waveguides used at millimeter wavelengths, or even higher frequencies up to the optical. Envisioned could be all electric nonreciprocal devices, in analogy to what g tensors could do in semiconductor heterostructures for electron spin control where the elimination of the external control magnetic field could allow all electric gating [4,5].

The simplest bicrystal heterostructure to study is the single period case shown in Fig. 1, with the guiding metal strip inserted between the two crystal layers causing

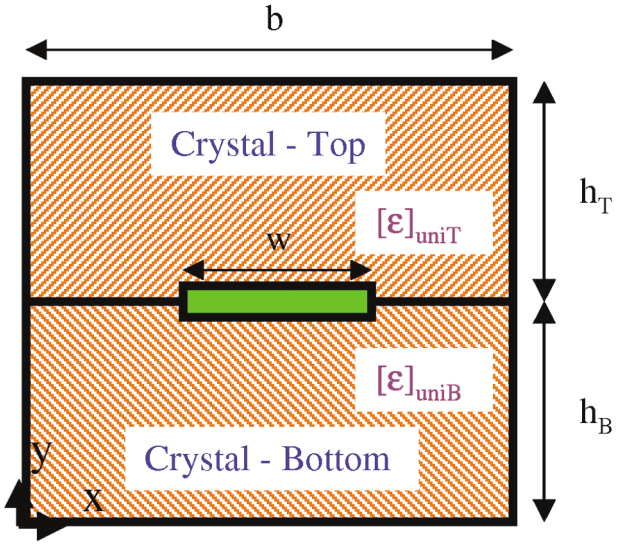

FIG. 1 (color). Cross section of the guided-wave stripline heterostructure consists of a single bicrystal period. Each crystal is positioned by rotations from the same principal axes tensor $\overline{\overline{\varepsilon}}$, denoted $[\varepsilon]_{uniA}$, $A = T$ (top), B (bottom).

fundamental mode propagation. Bottom and top crystal tensor permittivities are

$$\overline{\overline{\varepsilon}}_{b,t} = \begin{bmatrix} \varepsilon_{xx} & 0 & 0 \\ 0 & \varepsilon_{yy} & 0 \\ 0 & 0 & \varepsilon_{zz} \end{bmatrix} \tag{1}$$

in their principal axis systems, where two of the diagonal elements are the same. When they are rotated in the transverse xy plane normal to the z axis [6],

$$\overline{\overline{\varepsilon}}_{b,t} = \begin{bmatrix} [\varepsilon_{xx}\cos^2\theta_{b,t} + \varepsilon_{yy}\sin^2\theta_{b,t}] & [\varepsilon_{yy} - \varepsilon_{xx}](\sin 2\theta_{b,t})/2 & 0 \\ [\varepsilon_{yy} - \varepsilon_{xx}](\sin 2\theta_{b,t})/2 & [\varepsilon_{xx}\sin^2\theta_{b,t} + \varepsilon_{yy}\cos^2\theta_{b,t}] & 0 \\ 0 & 0 & \varepsilon_{zz} \end{bmatrix} \tag{2}$$

Rotation angle θ of the principal axes about the z axis is counterclockwise for positive angle. For a single layer of crystal, looking in the x principal axis direction appears the same as in the reverse direction. This is basically because marking off atomic layers in the $+x$ direction looks the same as marking them off in the $-x$ direction. However, when two crystals lie adjacent to each other, this is no longer generally true, since marking off atomic layers in the principal axis system of the bottom crystal, say in the x_b direction, will not mark off successive atomic layers in the x_t principal axis direction of the top crystal. The symmetry is broken.

One notices that the off-diagonal elements of $\overline{\overline{\varepsilon}}$ are maximized in the individual crystal layers when $\sin 2\theta = 1$. This occurs for $\theta = \pm 45°$. Choosing $\theta_b = +45°$ and $\theta_t = -45°$ allows both top and bottom crystals to have maximum off-diagonal elements. $\Delta\theta = \theta_b - \theta_t = 90°$ in this case. $\theta = 0°$ corresponds to the unrotated situation in (1), giving $\Delta\theta = \theta_b - \theta_t = 0°$. $\theta = \pm 90°$, setting $\theta_b = +90°$, and $\theta_t = -90°$ makes $\Delta\theta = \theta_b - \theta_t = 180°$. This last assignment causes the incommensurate marking off of atomic layers to vanish, making symmetry appear again (looks like the unrotated case again).

There are only two possibilities for (1) being a uniaxial tensor in the initial unrotated principal axes system. Dyadic tensors must be either

$$\overline{\overline{\varepsilon}}^{1}_{b,t} = \begin{bmatrix} \varepsilon_e & 0 & 0 \\ 0 & \varepsilon_o & 0 \\ 0 & 0 & \varepsilon_o \end{bmatrix} \quad \text{or}$$

$$\overline{\overline{\varepsilon}}^{2}_{b,t} = \begin{bmatrix} \varepsilon_o & 0 & 0 \\ 0 & \varepsilon_e & 0 \\ 0 & 0 & \varepsilon_o \end{bmatrix}, \tag{3}$$

because there are only two ways to insert the single extraordinary axis permittivity into the 2×2 submatrix, also forcing the last $\hat{z}\,\hat{z}$ diagonal dyadic element to be the ordinary value.

If $\theta = \pm 45°$ is chosen, with θ_b and θ_t as above, then $\sin^2\theta = \cos^2\theta = 1/2$, making the diagonal dyadic elements from (2) become

$$\varepsilon_{rxx} = \varepsilon_{ryy} = \frac{\varepsilon_{xx} + \varepsilon_{yy}}{2} \Rightarrow \varepsilon_a = \frac{\varepsilon_e + \varepsilon_o}{2}, \tag{4}$$

an averaged value of the first two principal axis diagonal dyadic elements. Off-diagonal dyadic elements from (2) become [for $\theta > 0$ case].

$$\varepsilon_{rxy} = \varepsilon_{ryx} = \frac{\varepsilon_{yy} - \varepsilon_{xx}}{2} \Rightarrow \varepsilon_{d1} = \frac{\varepsilon_o - \varepsilon_e}{2}, \quad \varepsilon_{d2} = \frac{\varepsilon_e - \varepsilon_o}{2}, \tag{5}$$

depending on whether the first $\overline{\overline{\varepsilon}}^{1}_{b,t}$ or second $\overline{\overline{\varepsilon}}^{2}_{b,t}$ dyadic is selected in (3). Positive crystal [7], defined as having $\varepsilon_e - \varepsilon_o > 0$ makes $\varepsilon_{d1} < 0$, and a negative crystal with $\varepsilon_e - \varepsilon_o < 0$ makes $\varepsilon_{d1} > 0$. Exactly the reverse happens for the second dyadic tensor, namely, $\varepsilon_e - \varepsilon_o > 0$ makes $\varepsilon_{d2} > 0$, and $\varepsilon_e - \varepsilon_o < 0$ makes $\varepsilon_{d2} < 0$.

Once the crystalline physics has been determined as above, then the physics based spectral domain method [8], and its use summarized in [2] with related references contained therein, may be used to specify the Green's function system matrix $\mathbf{R}$ which gives the tangential transverse field component variation (column vector $\aleph$) perpendicular to the heterostructure bilayers in the y direction:

$$\frac{d\aleph}{dy} = i\omega\mathbf{R}\aleph; \qquad \aleph = [E_x, E_z, H_x, H_z]^T. \tag{6}$$

Auxiliary equations give the two remaining field components, E_y and H_y. $\mathbf{R}$ is a 4×4 matrix, and its elements are given by

$$r_{11} = -\frac{\varepsilon_{yx}}{\varepsilon_{yy}}\frac{k_x}{\omega}, \qquad r_{12} = 0, \qquad r_{13} = \frac{1}{\varepsilon_{yy}}\frac{i\gamma k_x}{\omega^2}, \quad r_{14} = \mu - \frac{1}{\varepsilon_{yy}}\frac{k_x^2}{\omega^2}, \tag{7a}$$

$$r_{21} = -\frac{i\gamma}{\omega}\frac{\varepsilon_{yx}}{\varepsilon_{yy}}, \qquad r_{22} = 0, \qquad r_{23} = -\mu - \frac{1}{\varepsilon_{yy}}\frac{\gamma^2}{\omega^2}, \quad r_{24} = -\frac{1}{\varepsilon_{yy}}\frac{ik_x\gamma}{\omega^2}, \tag{7b}$$

$$r_{31} = -\frac{1}{\mu}\frac{i\gamma k_x}{\omega^2}, \qquad r_{32} = -\varepsilon_{zz} + \frac{1}{\mu}\frac{k_x^2}{\omega^2}, \quad r_{33} = 0, \qquad r_{34} = 0, \tag{7c}$$

$$r_{41} = \varepsilon_{xx} - \frac{\varepsilon_{xy}\varepsilon_{yx}}{\varepsilon_{yy}} + \frac{1}{\mu}\frac{\gamma^2}{\omega^2}, \qquad r_{42} = \frac{1}{\mu}\frac{ik_x\gamma}{\omega^2}, \quad r_{43} = \frac{i\gamma}{\omega}\frac{\varepsilon_{xy}}{\varepsilon_{yy}}, \qquad r_{44} = -\frac{k_x}{\omega}\frac{\varepsilon_{xy}}{\varepsilon_{yy}}, \tag{7d}$$

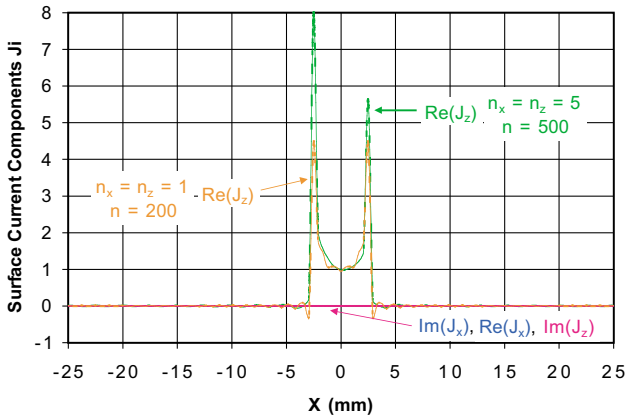

FIG. 2 (color). Surface current components J_i ($i = x, z$), are shown in terms of real and imaginary parts, versus x direction. Currents undergo the same inverse Fourier transform as fields back into the spatial domain. Only Re(J_z) exists for unrotated $\theta = 0°$ and rotated $\theta = \pm 45°$ crystal cases.

when $\overline{\overline{\varepsilon}}$ is uniaxial [elements are rotated (2) values given in (4) and (5)], $\overline{\overline{\mu}}$ is isotropic, and the optical activity tensors $\overline{\overline{\rho}}$ and $\overline{\overline{\rho}}'$ are null for the problem being treated here.

When no rotations are applied to the tensor $\overline{\overline{\varepsilon}}$ in (1), $\theta = 0°$ and the two separate crystals seem to be one uniform slab, with an insert of an infinitely thin, perfectly conducting metal guiding strip (see Fig. 1). In this case one would not expect the current distribution J_z along the x axis to have any asymmetry, as indeed found in Fig. 2. (Note that since small signal solutions are found, only relative values of **J** and **E** are important.) Dimensions of the structure shown in the figure were chosen to be $w = h_B = h_T = 5$ mm, $b = 50$ mm, making $b/w = 10$. Permittivity tensor was chosen to be the first type $\overline{\overline{\varepsilon}}^{\mathrm{I}}_{b,t}$, for a negative crystal with $\varepsilon_e = 4.5$ and $\varepsilon_o = 5.5$. Nominal permittivity is five ($\varepsilon_a = 5$) and this value was selected to be about the same as the nominal value of the YVO_4 positive crystal in [1] with $n_e = 2.25081$ and $n_o = 2.01768$ giving $\varepsilon_e = 5.06615$ and $\varepsilon_o = 4.07103$. The $\theta = 0°$ curve shown for J_z phasor (complex) component was found by using an equal number of even and odd parity current basis functions $n_x = n_z = 1$ for the currents J_x and J_z in the x and z directions. The number of spectral (Fourier) terms $n = 200$. The same result is obtained using only even parity current basis functions, since the fundamental mode studied here is a symmetric mode. Use of more current basis functions $n_x = n_z > 1$ produces the same shaped curve. The large b/w ratio employed here was done to make almost all of the electromagnetic energy exist in the region around the guiding strip, allowing the vertical sides walls (which are perfect conductors) to act as computational boundaries for the numerical solution. Because the electromagnetic fields to be presented next were constructed by taking the real part of the phasors (i.e., $E_{\mathrm{plot}} = |\mathrm{Re}\mathbf{E}|$), to obtain physical

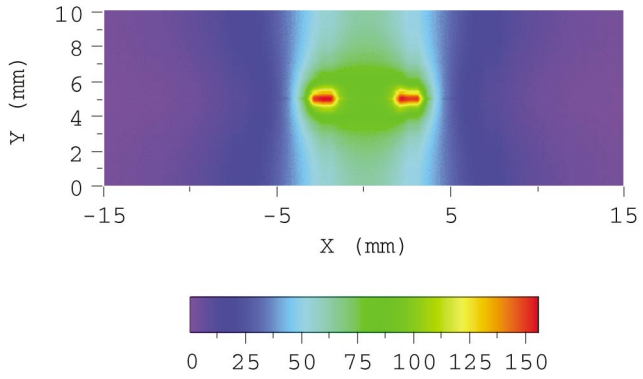

FIG. 3 (color). Electric field magnitude E distribution in the stripline heterostructure cross section is presented for the unrotated crystal case $\theta = 0°$.

quantities, the same operation pertains, of course, to the surface current.

Electromagnetic field distribution E for the magnitude of the rf electric field **E** is displayed in Fig. 3 for the $\theta = 0°$ unrotated case. Electric rf field distribution E is symmetric, extending between the bottom and top ground planes (which act as perfect conductors). The highest field intensity of E is at the strip edges, with an elliptic region of somewhat lower intensity surrounding the entire strip. Figure 4 shows the rotated case of $\theta = \pm 45°$ with

$$\overline{\overline{\varepsilon}}(\theta = \pm 45°) = \begin{bmatrix} 5 & \pm 0.5 & 0 \\ \pm 5 & 5 & 0 \\ 0 & 0 & 5.5 \end{bmatrix}. \qquad (8)$$

Clearly, the electric field distribution E is asymmetric, having shifted in a comet shaped pattern to the left. Figure 2 shows the J_z current distribution for this rotated case with $n_x = n_z = 5$ and $n = 500$ ($n_x = n_z = 1$ and $n = 200$ gave nearly the same curve shape, with almost the same ratio of the left and right peak currents at the strip edges). As further substantiation that the broken symmetry effect requires the paired heterostructure of

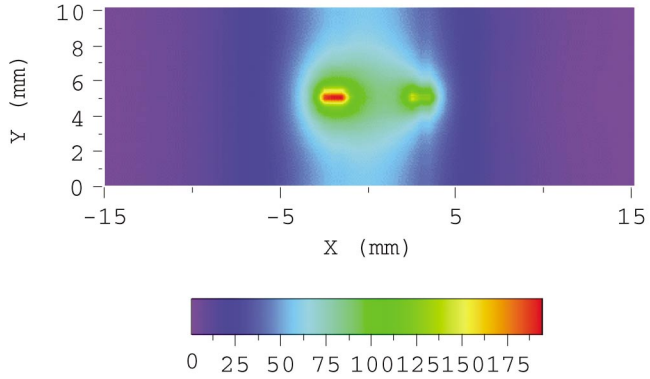

FIG. 4 (color). Electric field magnitude E distribution in the stripline heterostructure cross section is presented for the rotated crystal case $\theta = \pm 45°$.

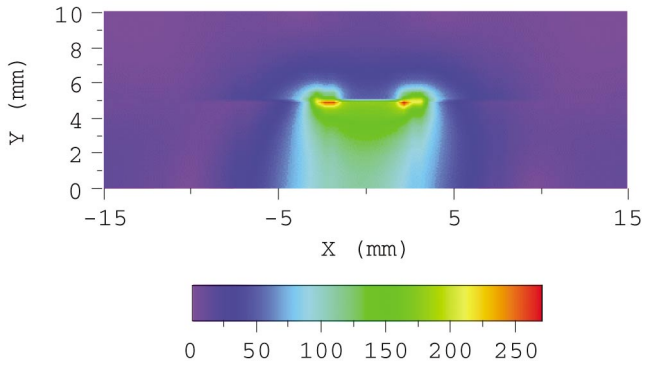

FIG. 5 (color). Electric field magnitude E distribution in the microstrip single crystal structure cross section is presented for the rotated crystal case $\theta = 45°$.

the bicrystal, Fig. 5 shows the field distribution for E when the structure is converted into a microstrip configuration by extirpating the crystal from the top, leaving only air. Bottom crystal still has the $\theta_b = +45°$ rotation. Using $n_x = n_z = 1$ and $n = 200$, and either even or both even and odd symmetry current basis functions, the same basically symmetric distribution is observed (slight distortion seen is an artifact of post processing). So it is concluded that a single crystal material or single layer will not produce the broken symmetry effect generating asymmetric field distributions.

It has been shown in this Letter that the broken symmetry created by a heterostructure bicrystal can lead to asymmetric electromagnetic field distributions. This is a very desirable effect, since the asymmetric disposition of the fields can allow waves traveling in opposite directions to see an enhanced field distribution to the left or right. Because the field displacement effect [9], relying on asymmetric fields in a guided wave structure, uses this effect to advantage by placing an absorbing nonconductive strip off-center from the guiding strip metal to dissipate the electromagnetic field energy for the wave propagating in one direction but not the opposite direction, one can envision the creation of isolator devices which do not rely on the spin precession effect found in ceramic ferrites.

*Email address: krowne@webbsight.nrl.navy.mil

[1] Y. Zhang, B. Fluegel, and A. Mascarenhas, Phys. Rev. Lett. **91**, 157404 (2003).
[2] C. M. Krowne, Phys. Rev. Lett. **92**, 053901 (2004).
[3] C. M. Krowne, IEEE Trans. Microwave Theory Tech. **51**, 2269 (2003).
[4] J. Levy, Phys. Rev. Lett. **89**, 147902 (2002).
[5] Y. Kato, R. C. Myers, D. C. Driscoll, A. C. Gossard, J. Levy, and D. D. Awschalom, Science **299**, 1201 (2003).
[6] C. M. Krowne, Microw. Opt. Technol. Lett. **28**, 63 (2001). Unitary matrix $L(\phi; z)$ in (24) of this reference must have $\phi \rightarrow 90° - \phi$ to have strictly the same rotation sense as the previous two in (24) about the x and y axes. Then the new rotated permittivity tensor is $\overline{\overline{\varepsilon}}' = \overline{\overline{L}}\,\overline{\overline{\varepsilon}}\,\overline{\overline{L}}^T$ where elements of $\overline{\overline{L}}$ are $L_{xx} = -L_{yy} = -\cos\theta$, and $L_{xy} = L_{yx} = \sin\theta$, where θ is exchanged for ϕ to agree with notation in (2) [and replaces (30) in this reference].
[7] J. F. Nye, *Physical Properties of Crystals* (Oxford Univ. Press, Oxford, U.K., 1979).
[8] C. M. Krowne, IEEE Trans. Microw. Theory Tech. **32**, 1617 (1984).
[9] F. J. Rosenbaum, *Integrated Ferrimagnetic Devices*, in Advances in Microwaves (Academic Press, New York, 1974), Vol. 8, page 203; J. D. Adam *et al.*, IEEE Trans. Microw. Theory Tech. **50**, 721 (2002); M. E. Hines, IEEE Trans. Microw. Theory Tech. **19**, 442 (1971); F. N. Bradley, *Materials for Magnetic Functions* (Hayden, New York, 1971); P. J. B. Clarricoats, *Microwave Ferrites* (Wiley, New York, 1961); R. F. Soohoo, *Theory & Applications of Ferrites* (Prentice-Hall, New Jersey, 1960). Note, for principal axis static bias $\mathbf{H}_0$ field, asymmetry occurs in a direction normal to $\mathbf{H}_0$ and propagation direction $\mathbf{k}_p$. The edge guided microstrip isolator uses $H_0\hat{x}$; the earlier waveguide structure used $H_0\hat{y}$.